PID Control of Biochemical Reaction Networks

Max Whitby, Luca Cardelli, Marta Kwiatkowska, Luca Laurenti, Mirco Tribastone, and Max Tschaikowski

***Abstract*—Principles of feedback control have been shown to naturally arise in biological systems and have been applied with success to build synthetic circuits. Here we present an implementation of a proportional-integral-derivative (PID) controller as a chemical reaction network with mass action kinetics. This makes the controller synthesizable *in vitro* using DNA strand displacement technology, owing to its demonstrated capability of realizing arbitrary reaction-network designs as interacting DNA molecules. Previous related work has studied biological PID architectures using linearizations of nonlinear dynamics arising in both the controller components and in the plant. In this paper we present a proof of correctness of our nonlinear design in closed loop using arguments from singular perturbation theory. As an application to show the effectiveness of our controller, we provide numerical simulations on a genetic model to perform PID feedback control of protein expression.**

***Index Terms*—Chemical process control, Biological systems, Modeling, Nonlinear systems**

I. Introduction

CHEMICAL Reaction Networks (CRNs) are a widely used formalism to describe biochemical systems [1]. More recently, they have also been employed in synthetic biology as the reference language for realizing circuits made of DNA [2], [3]. Due to the numerous potential applications ranging from smart therapeutics to biosensors, the construction of CRNs that exhibit prescribed dynamics is a major goal. However, this is difficult due the complexity of biological systems and limited knowledge of their dynamics [4], [5].

Negative feedback and proportional-integral-derivative (PID) controllers are widely used in control engineering due to their ability to achieve accurate set-point tracking and robustness to disturbances even with only partial knowledge of the system. Owing to these properties, such mechanisms have also been applied with success in synthetic biology [6], [7], also motivated by the fact that they naturally occur in living organisms [8]–[13].

In this work we present a CRN implementation of a PID controller using the so-called *dual rail* encoding in systems biology [14], whereby the value of a signal is represented as the difference between two nonnegative signals, each of which can in turn be directly represented by concentration levels of appropriately chosen biochemical species which are assumed to interact according to mass action kinetics. This is advantageous from a practical/technological viewpoint because any CRN with mass action kinetics has a translation scheme into a DNA strand displacement device [15], [16]. From a theoretical viewpoint, we prove the correctness of the PID controller in closed loop with a plant realized as a mass-action CRN (although our results carry over to plants given in terms of smooth control systems). Our proof is based on arguments from singular perturbation theory [17], establishing that the proportional, integrative and derivative components do apply the desired control in the limit when certain kinetic parameters of the CRN implementation go to infinity. In doing so we extend and formalize our previous conference paper [18]. There, the correctness was restricted to assuming each PID component in isolation in closed loop with the plant. In this paper the result is extended, and a full provided, for the whole PID design in closed loop. We also provide further numerical evidence of the effectiveness of this architecture on a gene expression example [19], [20], where we control the time evolution of a protein, which can diffuse from its original compartment, by acting on the expression of mRNA and we investigate the robustness of PID controlled to parameter noise.

There is previous work that has focused on simpler architectures with proportional and integral components only [13], [14], [21]. More closely related is the literature which also considers the derivative action. However, in closed loop it has been studied using transfer functions [22]–[26], and thus implicitly depends on a linearization of the nonlinear plant dynamics. In open loop, it has been analyzed for its noise suppression properties at steady state [27]. Instead, this paper presents the first analysis of the closed-loop system in the nonlinear setting to the best of our knowledge. While some works propose implementations using Hill semantics [22], [25], in a recent work [26]—which appeared independently of our previous conference version [18]—the authors present a similar approach to ours based on dual-rail encoding, motivated by the possibility to realize the design using DNA technology, with a major difference in the structure of the derivative block.

II. Biochemical Reaction Networks

Mass-action kinetics: A CRN $\mathcal{C} = (\mathcal{S}, \mathcal{R})$ is a pair of finite sets, where $\mathcal{S}$ is a set of species and $\mathcal{R}$ is a set of reactions. A reaction is a triple (ρ, α, π), where $\rho \in \mathbb{N}_0^{\mathcal{S}}$ are the *reagents*, $\pi \in \mathbb{N}_0^{\mathcal{S}}$ are the *products* and $\alpha \in \mathbb{R}_{>0}$ is the reaction rate coefficient. The components of vectors ρ and π represent the stoichiometries of the reaction. We denote the A-th coordinate of $\sigma \in \mathbb{N}_0^{\mathcal{S}}$ by σ_A; the zero vector in $\mathbb{N}_0^{\mathcal{S}}$ is denoted by $\varnothing$. A reaction will be written as

$$\sum_{A \in \mathcal{S}} \rho_A A \xrightarrow{\alpha} \sum_{A \in \mathcal{S}} \pi_A A,$$

M. Whitby performed this research while studying for doctorate at the University of Oxford and is now with Oxford Heartbeat, UK (mathemaxis@gmail.com). L. Cardelli, M. Kwiatkowska, and L. Laurenti, are with the University of Oxford, UK. ({*firstname.lastname*}@cs.ox.ac.uk). M. Tribastone is with IMT Lucca, Italy (mirco.tribastone@imtlucca.it). M. Tschaikowski is with Aalborg University, Denmark (tschaikowski@cs.aau.dk).

This work was supported in part by the Italian Ministry of Research, grant 2017TWRCNB, and the Danish Poul Due Jensen Foundation, grant 883901. L.C. was supported by a Royal Society Research Professorship.

where zero components are omitted.

We consider the well-known reaction-rate equations with mass-action kinetics. Given a CRN $\mathcal{C} = (\mathcal{S}, \mathcal{R})$ and an initial condition $\bar{x} \in \mathbb{R}^{\mathcal{S}}_{\geq 0}$ representing the initial concentration of each species, the time course of the concentrations can be described as the solution of an initial value problem with the following system of ODEs

$$\partial_t x_A(t) = \sum_{(\rho,\alpha,\pi)\in\mathcal{R}} (\pi_A - \rho_A) \cdot \alpha \cdot \prod_{B\in\mathcal{S}} x_B(t)^{\rho_B}, \quad (1)$$

and initial condition $x(0) = \bar{x}$. For a species $A \in \mathcal{S}$ we denote by $x_A(t)$, or x_A when the time dependence is clear from the context, the concentration of A at time t.

Dual rail encoding: The solutions to (1) are non-negative if the initial conditions are. However, a PID controller might involve negative quantities such as the error difference between the set-point and the output, as well as its derivative. In the dual rail encoding [14], a signal is decomposed into a "positive" and "negative" species component obeying mass action kinetics, whilst such that each individual species concentrations cannot be negative. For a signal A we denote the two distinct component species by A^+ and A^-, i.e., A is given by the difference $A^+ - A^-$. Reactions of the form $A^+ + A^- \to \varnothing$ keep the concentrations bounded.

Graphical representation: Throughout the paper we will use a compact formal representation of CRNs based on a graphical notation as a labelled directed bipartite graph, according to the Petri net representation with species and reaction nodes [28]. A reaction node is a square labelled with a rate coefficient. A species node is a circle labelled with a species name. There is an edge from a species node to a reaction node if the species is a reagent of the reaction; similarly, an edge from a reaction node to a species node indicates a product of the reaction. For example, we have the following representation for the reaction $2A + B \xrightarrow{\alpha} B + 2C$:

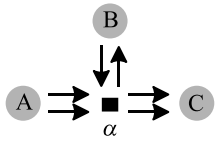

$$\equiv \quad 2A + B \xrightarrow{\alpha} B + 2C$$

Throughout the rest of the paper, for ease of presentation we do not draw labels on edges if the related multiset multiplicity is 1. We also remove the black box representing reaction nodes to reduce clutter. Finally, we introduce a short-hand notation for recurring reaction patterns as shown in Figure 1, where each arc is either a pointed arrow (↑) or a rounded arrow ❣ with the source represented by the flat edge and the target represented by the arrow head. A pointed arrow represents a normal reaction between reactants and products, and a rounded arrow represents a *catalyst*, i.e., a species C with positive stoichiometry in a reaction $\rho \xrightarrow{\alpha} \pi$ such that $\rho_C = \pi_C$.

III. CRN implementation of the PID controller

We introduce the CRN implementation of the proportional, integral, and derivative components of a PID controller. As illustrated in Figure 2, we describe them as blocks where the incoming species are $E^{\pm}$ (which will indicate the dual-rail error signal between the species representing the set-point R and the plant output Y). The output of the PID controller is denoted by $U^{\pm}$.

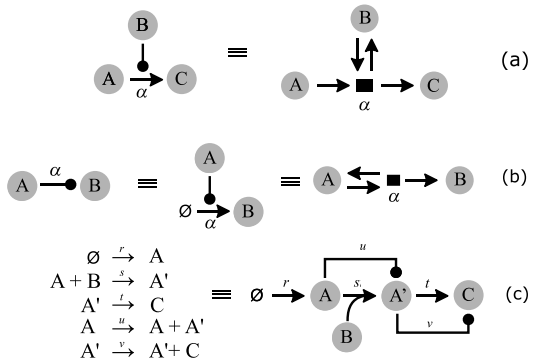

Figure 1: Short-hand CRN graphical notation. (a) A catalytic bi-molecular reaction $A + B \to B + C$ as an equivalent Petri net; (b) a catalytic uni-molecular reaction $A \to A + B$; (c) a sample CRN depicted using the short-hand notation (with some square nodes omitted).

Let $(\mathcal{S}_\Sigma, \mathcal{R}_\Sigma)$ denote the mass-action CRN representing the plant. We construct a CRN encoding of a PID feedback law as indicated in Figure 2. For the benefit of presentation, we focus on one-dimensional controls, since the discussion generalises to the multidimensional case in a straightforward manner. The CRN encoding is given by the following components:

- subtraction block $(\mathcal{S}^{\mathbf{M}}, \mathcal{R}^{\mathbf{M}})$;
- addition block $(\mathcal{S}^{\mathbf{A}}, \mathcal{R}^{\mathbf{A}})$;
- proportional block $(\mathcal{S}^{\mathbf{P}}, \mathcal{R}^{\mathbf{P}})$, with gain r_P;
- integral block $(\mathcal{S}^{\mathbf{I}}, \mathcal{R}^{\mathbf{I}})$, with gain r_I;
- derivative block $(\mathcal{S}^{\mathbf{D}}, \mathcal{R}^{\mathbf{D}})$, with gain r_D.

where the **P**, **I** and **D** blocks can be removed by setting their gains to zero. With this, the overall CRN is given by

$$(\mathcal{S}_\Sigma, \mathcal{R}_\Sigma) \cup (\mathcal{S}_F, \mathcal{R}_F), \quad (2)$$

where the feedback law CRN is defined by

$$(\mathcal{S}_F, \mathcal{R}_F) = \bigcup_{X\in\mathcal{X}} (\mathcal{S}^X, \mathcal{R}^X), \qquad \mathcal{X} = \{\mathbf{M}, \mathbf{A}, \mathbf{P}, \mathbf{I}, \mathbf{D}\}.$$

We now detail each of the blocks in Figure 2. Following [14], we first discuss the addition, subtraction, proportional and integral blocks in Section III-A. In Section III-B we present the derivative block. The formal correctness of all blocks is shown by means of singular perturbation theory in Section V, instead. That is, we show that for the feedback loop in Figure 2 and any plant, the proportional, derivative, and integral block are computing the correct functions.

A. Subtraction, Addition, Proportional and Integral Blocks

Definition 1 (Subtraction/minus block, Fig. 2(M))**.** *For incoming species R^+, R^-, Y, outgoing species E^+, E^- and parameters $s_M, q \in \mathbb{R}_{>0}$, the* subtraction block *is the CRN composed by the following reactions*

$$Y \xrightarrow{s_M} Y + E^+ \qquad R^- \xrightarrow{s_M} R^- + E^+ \qquad R^+ \xrightarrow{s_M} R^+ + E^-$$
$$E^+ + E^- \xrightarrow{q} \varnothing \qquad E^+ \xrightarrow{s_M} \varnothing \qquad E^- \xrightarrow{s_M} \varnothing$$

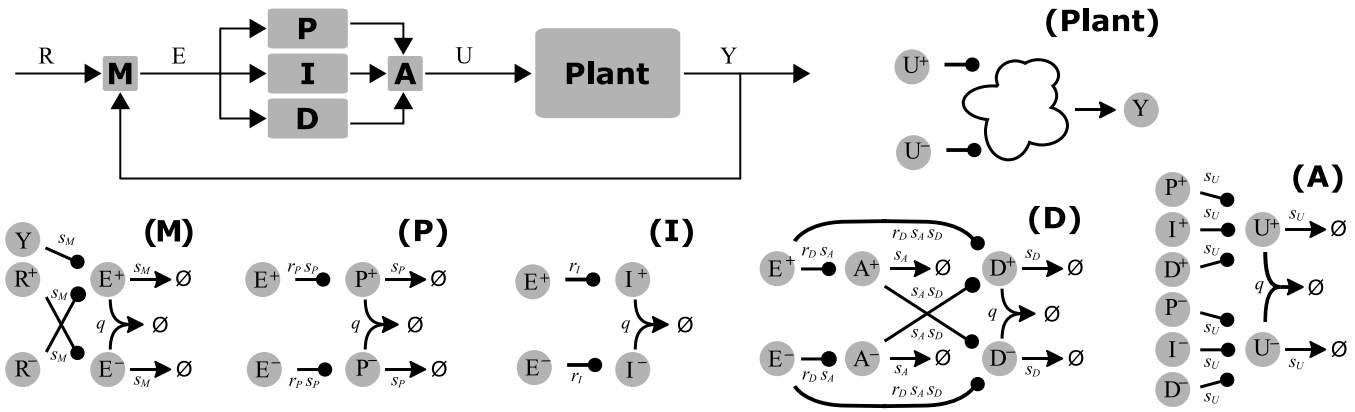

Figure 2: We present our feedback loop (top left) which takes a smooth reference signal R (in dual rail in its most general case) and, along with the feedback Y, produces an error E computed as $Y - R$. Signal E is obtained by the subtraction block **(M)**, and is fed to the controller, the chemical composition of which is described in **(P)**,**(I)**,**(D)**. The proportional and integral blocks **(P)**,**(I)** are taken from [14]. The proportional block returns the product $r_P x_E$ for a given x_E and $r_P \geq 0$, while the integral block takes an incoming signal x_E and computes the outgoing signal $r_I \int_0^t x_E(\tau)d\tau$ for some gain factor $r_I \geq 0$. Instead, the novel derivative block **(D)** takes an incoming signal x_E and produces the outgoing signal $r_D \partial_t x_E$, where $r_D \geq 0$ is again a gain factor. The foregoing blocks are summed by the addition block **(A)**, yielding a control signal x_U which steers the plant by the CRN encoding presented in Section III. As a result, the plant **(Plant)** produces a signal Y that is fed back as a single-rail signal. The presence of gain factors in each block allows one to adjust the weights of each block.

The addition block is given by the following reactions.

Definition 2 (Three-Way addition block [14], Fig. 2(A))**.** *For incoming species P^+, I^+, D^+ and P^-, I^-, D^-, outgoing species U^+, U^-, and parameters $s, q \in \mathbb{R}_{>0}$ the* addition block *is a CRN composed by the following reactions*

$$P^+ \xrightarrow{s_U} P^+ + U^+ \quad I^+ \xrightarrow{s_U} I^+ + U^+ \quad D^+ \xrightarrow{s_U} D^+ + U^+$$
$$P^- \xrightarrow{s_U} P^- + U^- \quad I^- \xrightarrow{s_U} I^- + U^- \quad D^- \xrightarrow{s_U} D^- + U^-$$
$$U^+ + U^- \xrightarrow{q} \varnothing \quad U^+ \xrightarrow{s_U} \varnothing \quad U^- \xrightarrow{s_U} \varnothing$$

We next provide the proportional block which computes an outgoing signal that is proportional to the incoming signal.

Definition 3 (Proportional block [14], Fig. 2(P))**.** *For incoming species E^+, E^-, outgoing species P^+, P^-, parameters $s_P, q \in \mathbb{R}_{>0}$, and the gain factor $r_P \in \mathbb{R}_{\geq 0}$, the* proportional block *is a CRN composed by the following reactions*

$$E^+ \xrightarrow{r_P s_P} E^+ + P^+ \qquad E^- \xrightarrow{r_P s_P} E^- + P^-$$
$$P^+ + P^- \xrightarrow{q} \varnothing \qquad P^+ \xrightarrow{s_P} \varnothing$$
$$P^- \xrightarrow{s_P} \varnothing$$

The integral component computes a multiple of the integral of the incoming signal.

Definition 4 (Integral block [14], Fig. 2(I))**.** *For incoming species E^+, E^-, outgoing species I^+, I^-, parameter $q \in \mathbb{R}_{>0}$ and gain factor $r_I \in \mathbb{R}_{\geq 0}$, the integral block is given by the following CRN*

$$E^+ \xrightarrow{r_I} E^+ + I^+ \quad E^- \xrightarrow{r_I} E^- + I^- \quad I^+ + I^- \xrightarrow{q} \varnothing$$

B. Derivative Block

Building a derivative module by chemical reactions is challenging because differentiation can only be done by comparing a signal at two time points, inherently requiring an approximation dependent on the time difference. This is resolved by the network in Figure 2 (D), which handles dual rail signals. Intuitively, the incoming signals E^+ and E^- are sampled at two time points, E^+, A^+ and E^-, A^-, respectively, and a multiple of their difference is provided via D^+, D^-. In Figure 2 (D), the three reactions

$$E^+ \xrightarrow{r_D s_A s_D} E^+ + D^+, \quad A^- \xrightarrow{s_A s_D} A^- + D^+, \quad D^+ \xrightarrow{s_D} \varnothing$$

imply $x_{D^+} \approx r_D s_A x_{E^+} + s_A x_{A^-}$ when s_D is large. In a similar fashion, the symmetric three reactions ensure that $x_{D^-} \approx r_D s_A x_{E^-} + s_A x_{A^+}$, allowing us thus to obtain

$$x_{D^+} - x_{D^-} \approx s_A(r_D x_{E^+} + x_{A^-}) - s_A(r_D x_{E^-} + x_{A^+}) \quad (3)$$

for large s_D. The above conclusion anticipates Theorem 1 from Section V and separates the fast and very fast time scales. Assuming that (3) when $s_D \to \infty$, we next anticipate Theorem 2 from Section V that separates the slow and fast time scale. To this end, we first note that the two reactions

$$E^+ \xrightarrow{r_D s_A} E^+ + A^+ \qquad \text{and} \qquad A^+ \xrightarrow{s_A} \varnothing$$

imply $x_{A^+} \approx r_D x_{E^+}$ for large s_A. In fact, since x_{A^+} tracks $r_D x_{E^+}$ with a delay that is reciprocal to s_A, we can approximate $\partial_t r_D x_{E^+}$ by $r_D x_{E^+} - x_{A^+}$ when s_A is large. The symmetric two reactions imply in a similar manner that $\partial_t r_D x_{E^-} \approx r_D x_{E^-} - x_{A^-}$ when $s_A \to \infty$. Since $s_D \to \infty$ was considered before $s_A \to \infty$, it intuitively holds true that $1 \ll s_A \ll s_D$ and we obtain the time scales slow, fast and very fast, respectively. The overall discussion motivates the approximation

$$\begin{aligned} x_{D^+} - x_{D^-} &\approx s_A(r_D x_{E^+} + x_{A^-}) - s_A(r_D x_{E^-} + x_{A^+}) \\ &= s_A(r_D x_{E^+} - x_{A^+}) - s_A(r_D x_{E^-} - x_{A^-}) \\ &\approx \partial_t r_D x_{E^+} - \partial_t r_D x_{E^-} \end{aligned}$$

Definition 5 (Derivative block, Fig. 2(D))**.** *For incoming species E^+, E^-, auxiliary species A^+, A^-, outgoing species D^+, D^-, parameters $q, s_D, s_A \in \mathbb{R}_{>0}$ and gain factor $r_D \in \mathbb{R}_{\geq 0}$, the derivative block is a CRN composed by the following reactions*

$$
\begin{aligned}
E^+ &\xrightarrow{r_D s_A} E^+ + A^+ & E^- &\xrightarrow{r_D s_A} E^- + A^- \\
E^+ &\xrightarrow{r_D s_A s_D} E^+ + D^+ & E^- &\xrightarrow{r_D s_A s_D} E^- + D^- \\
A^+ &\xrightarrow{s_A} \varnothing & A^- &\xrightarrow{s_A} \varnothing \\
A^+ &\xrightarrow{s_A s_D} A^+ + D^- & A^- &\xrightarrow{s_A s_D} A^- + D^+ \\
D^+ &\xrightarrow{s_D} \varnothing & D^- &\xrightarrow{s_D} \varnothing \\
D^+ + D^- &\xrightarrow{q} \varnothing
\end{aligned}
$$

The correctness results provided in Section V ensure that the feedback loop depicted in Figure 2 converges, as all scaling parameters s approach infinity, to the solution of a limit ODE system which arises from Figure 2 when all component blocks **(M)**, **(P)**, **(I)**, **(D)** and **(A)** are replaced with the respective mathematical operations (i.e., substraction, multiplication, integration, differentiation and addition). By doing so, we extend [18] which established correctness only when exactly one component was replaced with its mathematical operation.

IV. Biochemical Implementation of CRNs

The chemical reaction networks we have described in Section III are abstract, in the sense that we do not specify what the chemical species may represent. A priori, there is no reason to believe that chemical species that obey those precise reactions may exist.

There are currently at least three approaches to assigning chemical species to such abstract networks. In Synthetic Biology one looks for naturally occurring biological molecules, typically genes and proteins, and modifies them and adapts them as needed by genetic engineering or artificial evolution. This is hard, because proteins are not easy to engineer from scratch, their reactions obey complex kinetic laws due to their complex structure, and their reaction rates are not easily predictable from their structure, and fall within restricted ranges. Moreover, the desired reactions need to execute in the largely unknown context of a living cell, competing for energy. Here one seeks to optimize the desired functionality starting from proteins and enzymes that are well studied and readily available, based on the principles of enzyme kinetics. Such is the case for example for the PID controller of [25], whose implementation and mathematical analysis is based on variations of Michaelis-Menten enzymatic kinetics.

A different approach comes from Molecular Programming, where the chemical species are in principle completely synthetic and not of biological origin, although DNA (natural or synthetic) is commonly used. The reactions typically run in-vitro in completely controlled environments with no unknown components, with the eventual goal of embedding them in living cells, or in other deployable physical media.

A third, intermediate, approach is to pick a few well characterized components and energy sources of biological origin, and use them in a uniform way in controlled in-vitro environments. This works extremely well due to the reliable and robust performance of naturally evolved biological components, such as polymerases and other enzymes, although the way the components themselves work is still only partially understood and only partially adaptable [29].

We focus here on a molecular programming approach based on *toehold mediated DNA strand displacement* [30], which is a kind of reaction between relatively short DNA strands that is unnatural, or thought to occur rarely in nature. The species of our abstract chemical reaction networks are each represented by an arbitrary (but carefully chosen) DNA strand; their reactions are designed to obey exactly the abstract reactions that the species are supposed to engage with. No other chemicals are used, except suitable buffer solutions, and no external energy source is provided: the reactions run down thermodynamically from the initial molecule populations. It has been shown that any CRN (any finite set of abstract chemical reactions with mass action kinetics, up to time rescaling) can be systematically compiled to such DNA molecules [31], which can then be produced by DNA synthesis or by bacterial cloning. The number of species is in principle unbounded, just by using longer strands for their encoding. Each abstract reaction is compiled to a sequence of DNA strand displacement operations, but the scheme can readily approximate to an arbitrary degree the mass action kinetics used in Section III [31]. Because of uniform architecture, the reaction rates are naturally equal for all reactions with the same number or reagents. It is also known experimentally that the reaction rates can be tuned across multiple orders of magnitudes [30], both in large exponential steps by modifying toehold lengths, and in small tuning steps by choosing particular strand sequences. The reaction rates are largely predictable by models of DNA structure [32], although in practice they are then tuned experimentally. This approach has been demonstrated experimentally, including, e.g., systems where 3 abstract reactions must have the same rates to a good approximation [3], [33]. The challenges in this area are to scale up the speed and number of concurrent reactions, with systems with over 100 distinct interacting sequences being demonstrated [34]. Moreover, there are significant challenges in deploying any DNA-based structures in-vivo, requiring isolation methods [35], or switching from DNA to RNA [36] or switching from DNA to artificial polymers that a cell would not interfere with [37]. In summary, biochemical implementation of CRNs is an active area of research, with solid theoretical, scientific, and engineering foundations, and with excellent prospects. We currently rely on approaches based on systematic compilation of CRNs, and on mass-action kinetics.

V. Asymptotic Correctness

Let Σ_0 be given by $\mathcal{S}_\Sigma = \Sigma_0 \dot\cup \{U^+, U^-\}$, and let $(\partial_t x_{\Sigma_0}, \partial_t x_{U^+}, \partial_t x_{U^-}) = \big(f_{\Sigma_0}(x_{\Sigma_0}, x_{U^+}, x_{U^-}), 0, 0\big)$ denote the ODE system associated to the plant CRN $(\mathcal{S}_\Sigma, \mathcal{R}_\Sigma)$ from (2). Note that on its own, i.e., without the PID feedback loop in place, the ODEs of the plant are such that x_{U^+}, x_{U^-} have zero derivatives. This essentially reflects that x_{U^+}, x_{U^-}

are plant parameters, rather than plant states. Because of this, we refer to x_{Σ_0} as the state vector of the plant.

Formally, the output of the plant, Y, is the coordinate x_Y of the state vector x_{Σ_0}. Moreover, the ODE system describing the entire PID feedback control loop is given by

$$\begin{aligned}
\partial_t x_{\Sigma_0} &= f_{\Sigma_0}(x_{\Sigma_0}, x_{U^+}, x_{U^-}) \\
\partial_t x_{E^+} &= s_M(x_Y + x_{R^-} - x_{E^+}) - q x_{E^+} x_{E^-} \\
\partial_t x_{E^-} &= s_M(x_{R^+} - x_{E^-}) - q x_{E^+} x_{E^-} \\
\partial_t x_{P^+} &= s_P(r_P x_{E^+} - x_{P^+}) - q x_{P^+} x_{P^-} \\
\partial_t x_{P^-} &= s_P(r_P x_{E^-} - x_{P^-}) - q x_{P^+} x_{P^-} \\
\partial_t x_{I^+} &= r_I x_{E^+} - q x_{I^+} x_{I^-} \\
\partial_t x_{I^-} &= r_I x_{E^-} - q x_{I^+} x_{I^-} \\
\partial_t x_{A^+} &= s_A(r_D x_{E^+} - x_{A^+}) \\
\partial_t x_{A^-} &= s_A(r_D x_{E^-} - x_{A^-}) \\
\partial_t x_{D^+} &= s_D\big(s_A(r_D x_{E^+} + x_{A^-}) - x_{D^+}\big) - q x_{D^+} x_{D^-} \\
\partial_t x_{D^-} &= s_D\big(s_A(r_D x_{E^-} + x_{A^+}) - x_{D^-}\big) - q x_{D^+} x_{D^-} \\
\partial_t x_{U^+} &= s_U x_{P^+} + s_U x_{I^+} + s_U x_{D^+} - s_U x_{U^+} - q x_{U^+} x_{U^-} \\
\partial_t x_{U^-} &= s_U x_{P^-} + s_U x_{I^-} + s_U x_{D^-} - s_U x_{U^-} - q x_{U^+} x_{U^-}.
\end{aligned} \tag{4}$$

With (4) at hand, we are ready to state our first result.

Theorem 1. *If $q > 0$ and $s_A > 0$ are held fixed, while $s_M = \kappa_M s$, $s_P = \kappa_P s$, $s_D = \kappa_D s$ and $s_U = \kappa_U s$ for positive constants $\kappa_M, \kappa_P, \kappa_D, \kappa_U$, then, as $s \to \infty$, the solution of (4) converges pointwise on interval $[0;T]$ to the solution of the limit system*

$$\begin{aligned}
\partial_t x_{\Sigma_0} &= f_{\Sigma_0}(x_{\Sigma_0}, x_{U^+}, x_{U^-}) \\
x_{E^+} &= x_Y + x_{R^-} \\
x_{E^-} &= x_{R^+} \\
x_{P^+} &= r_P x_{E^+} \\
x_{P^-} &= r_P x_{E^-} \\
\partial_t x_{I^+} &= r_I x_{E^+} - q x_{I^+} x_{I^-} \\
\partial_t x_{I^-} &= r_I x_{E^-} - q x_{I^+} x_{I^-} \\
\partial_t x_{A^+} &= s_A(r_D x_{E^+} - x_{A^+}) \\
\partial_t x_{A^-} &= s_A(r_D x_{E^-} - x_{A^-}) \\
x_{D^+} &= s_A(r_D x_{E^+} + x_{A^-}) \\
x_{D^-} &= s_A(r_D x_{E^-} + x_{A^+}) \\
x_{U^+} &= x_{P^+} + x_{I^+} + x_{D^+} \\
x_{U^-} &= x_{P^-} + x_{I^-} + x_{D^-},
\end{aligned} \tag{5}$$

if it admits a solution and the reference trajectories x_{R^+}, x_{R^-} are continuously differentiable on $[0;T]$.

Proof of Theorem 1. We interpret x_{E^+}, x_{E^-}, x_{P^+}, x_{P^-}, x_{D^+}, x_{D^-}, x_{U^+} and x_{U^-} as fast variables in the sense of Tikhonov's theorem [17, Section 8.2]. Consequently, the fast system is given by

$$\begin{aligned}
\partial_t x_{E^+} &= \kappa_M s(x_Y + x_{R^-} - x_{E^+}) \\
\partial_t x_{E^-} &= \kappa_M s(x_{R^+} - x_{E^-}) \\
\partial_t x_{P^+} &= \kappa_P s(r_P x_{E^+} - x_{P^+}) \\
\partial_t x_{P^-} &= \kappa_P s(r_P x_{E^-} - x_{P^-}) \\
\partial_t x_{D^+} &= \kappa_D s\big(s_A(r_D x_{E^+} + x_{A^-}) - x_{D^+}\big) \\
\partial_t x_{D^-} &= \kappa_D s\big(s_A(r_D x_{E^-} + x_{A^+}) - x_{D^-}\big) \\
\partial_t x_{U^+} &= \kappa_U s(x_{P^+} + x_{I^+} + x_{D^+} - x_{U^+}) \\
\partial_t x_{U^-} &= \kappa_U s(x_{P^-} + x_{I^-} + x_{D^-} - x_{U^-})
\end{aligned}$$

Note that slow variables in the sense of Tikhonov's theorem, i.e., x_{Σ_0}, x_{I^+}, x_{I^-}, x_{A^+}, x_{A^-} and the reference signal x_{R^+} and x_{R^-} are treated as constants in the fast system, while all terms that are not multiplied by the scaling parameter s are dropped (e.g., $-q x_{E^+} x_{E^-}$). With this, the fast system is linear and admits the unique equilibrium

$$\begin{aligned}
x_{E^+} &= x_Y + x_{R^-} \\
x_{E^-} &= x_{R^+} \\
x_{P^+} &= r_P x_{E^+} \\
x_{P^-} &= r_P x_{E^-} \\
x_{D^+} &= s_A(r_D x_{E^+} + x_{A^-}) \\
x_{D^-} &= s_A(r_D x_{E^-} + x_{A^+}) \\
x_{U^+} &= x_{P^+} + x_{I^+} + x_{D^+} \\
x_{U^-} &= x_{P^-} + x_{I^-} + x_{D^-}.
\end{aligned}$$

Since the linear system can be expressed using an upper triangular coefficient with diagonal

$$\big(-\kappa_M s, -\kappa_M s, -\kappa_P s, -\kappa_P s, -\kappa_D s, -\kappa_D s, -\kappa_U s, -\kappa_U s\big)^T,$$

the coefficient matrix admits only negative eigenvalues. This, in turn, ensures that the unique equilibrium from above is a global attractor of the fast system. With this, Tikhonov's theorem [17, Section 8.2] yields the statement. □

The next result assumes that a) the dynamics of the plant can be restated in terms of the difference signal $x_U = x_{U^+} - x_{U^-}$ and that b) the dynamics of the output is independent of x_U. While this limits the way how control signals can act on the plant (e.g., by the second assumption, the plant output cannot be actuated directly by the PID controller), various actuation schema satisfy both assumptions, see Section VI.

Theorem 2. *Defining the difference signal of species A by $x_A := x_{A^+} - x_{A^-}$, let us assume that the limit system (5) can be written as*

$$\begin{aligned}
\partial_t x_{\Sigma_0} &= g(x_{\Sigma_0}, x_U) \\
x_E &= x_Y - x_R \\
x_P &= r_P x_E \\
\partial_t x_I &= r_I x_E \\
\partial_t x_A &= s_A(r_D x_E - x_A) \\
x_D &= s_A(r_D x_E - x_A) \\
x_U &= x_P + x_I + x_D
\end{aligned} \tag{6}$$

That is, there exists a continuously differentiable function g such that

$$g(x_{\Sigma_0}, x_U) = f_{\Sigma_0}(x_{\Sigma_0}, x_{U^+}, x_{U^-}).$$

Moreover, assume that g_Y does not depend on x_U. Then, if $s_A \to \infty$, the solution of system (6) converges pointwise on interval $[0;T]$ to the solution of the limit system

$$\begin{aligned} \partial_t x^*_{\Sigma_0} &= g(x^*_{\Sigma_0}, x^*_U) \\ x^*_E &= x^*_Y - x_R \\ x^*_P &= r_P x^*_E \\ \partial_t x^*_I &= r_I x^*_E \\ x^*_D &= r_D \partial_t x^*_E \\ x^*_U &= x^*_P + x^*_I + x^*_D, \end{aligned} \tag{7}$$

whenever (6) admits a solution and the reference trajectory x_R is twice continuously differentiable on $[0;T]$.

Proof of Theorem 2. The key idea is to extend the system by the differential equation of x_D and to apply Tikhonov's theorem on the extended system. Specifically, differentiating x_D yields

$$\begin{aligned} \partial_t x_{\Sigma_0} &= g(x_{\Sigma_0}, x_U) \\ x_E &= x_Y - x_R \\ x_P &= r_P x_E \\ \partial_t x_I &= r_I x_E \\ \partial_t x_A &= s_A(r_D x_E - x_A) \\ x_D &= s_A(r_D x_E - x_A) \\ \partial_t x_D &= s_A\big(r_D \partial_t x_E - x_D\big) \\ x_U &= x_P + x_I + x_D \end{aligned}$$

Then, together with

$$h(x_{\Sigma_0}, x_I, x_D, x_R) := g(x_{\Sigma_0}, r_P(x_Y - x_R) + x_I + x_D),$$

an iterative application of the algebraic equations

$$\begin{aligned} x_E &= x_Y - x_R \\ x_P &= r_P x_E \\ x_D &= s_A(r_D x_E - x_A) \\ x_U &= x_P + x_I + x_D \end{aligned}$$

allows us to rewrite the system as

$$\begin{aligned} \partial_t x_{\Sigma_0} &= h(x_{\Sigma_0}, x_I, x_D, x_R) \\ \partial_t x_I &= r_I(x_Y - x_R) \\ \partial_t x_A &= s_A(r_D(x_Y - x_R) - x_A) \\ \partial_t x_D &= s_A r_D\big(h_Y(x_{\Sigma_0}, x_I, x_D, x_R) - \partial_t x_R\big) - s_A x_D \end{aligned}$$

By interpreting x_A, x_D as fast and x_{Σ_0}, x_I, x_R as slow variables, the fast system is given by

$$\begin{aligned} \partial_t x_A &= s_A(r_D(x_Y - x_R) - x_A) \\ \partial_t x_D &= s_A r_D\big(h_Y(x_{\Sigma_0}, x_I, x_D, x_R) - \partial_t x_R\big) - s_A x_D \end{aligned}$$

By assumption, h_Y does not depend on x_D because it does not depend on x_U. Hence, the term $h_Y(x_{\Sigma_0}, x_I, x_D, x_R)$ acts as a constant, thus implying that the fast system is linear with unique global attractor

$$\begin{aligned} x_A &= r_D(x_Y - x_R) \\ x_D &= r_D\big(h_Y(x_{\Sigma_0}, x_I, x_D, x_R) - \partial_t x_R\big) \end{aligned}$$

This allows us to obtain the claim by using Tikhonov's theorem [17, Section 8.2]. □

By combining both preceding theorems, we can state our main result.

Theorem 3. *Assume that the reference signal (x_{R^+}, x_{R^-}) is twice continuously differentiable and that systems (4)-(7) admit unique solutions on $[0;T]$ for given initial conditions satisfying $x_{\Sigma_0}(0) = x^*_{\Sigma_0}(0)$. Then, for any $t \in [0;T]$ and $\eta > 0$, there exist $s > 0$ and $s_A > 0$ such that the solutions of (4) and (7) satisfy*

$$\|x_{\Sigma_0}(t) - x^*_{\Sigma_0}(t)\| \le \eta,$$

provided that $s_M = \kappa_M s$, $s_P = \kappa_P s$, $s_D = \kappa_D s$ and $s_U = \kappa_U s$ in (4).

Proof of Theorem 3. By Theorem 2, we can pick an $s_A > 0$ such that

$$\|x^*_{\Sigma_0}(t) - \hat{x}_{\Sigma_0}(t)\| \le \eta/2,$$

where $\hat{x}_{\Sigma_0}$ refers to the solution of (6). Moreover, thanks to Theorem 1, for the just fixed $s_A > 0$ there exists an $s > 0$ satisfying

$$\|x_{\Sigma_0}(t) - \tilde{x}_{\Sigma_0}(t)\| \le \eta/2,$$

where $x_{\Sigma_0}(t)$ and $\tilde{x}_{\Sigma_0}(t)$ refers to the solution of (4) and (5), respectively. Since $\tilde{x}_{\Sigma_0}(t) = \hat{x}_{\Sigma_0}(t)$, the triangle inequality yields the claim. □

It appears that the correctness of the derivative component cannot be inferred by using two instead of three time scales. To see this and to allow for a better comparison with related work, let us assume that $s_A = 1/\varepsilon_A$ and $s_D = 1/\varepsilon_D$ for small $\varepsilon_A, \varepsilon_D > 0$. With this, the differential equation of x_{D^+}

$$\partial_t x_{D^+} = s_D\big(s_A(r_D x_{E^+} + x_{A^-}) - x_{D^+}\big) - q x_{D^+} x_{D^-}$$

rewrites as

$$\varepsilon_D \varepsilon_A \partial_t x_{D^+} = \underbrace{(r_D x_{E^+} + x_{A^-}) - \varepsilon_A x_{D^+} - \varepsilon_D \varepsilon_A q x_{D^+} x_{D^-}}_{F_{D^+}(x_{E^+}, x_{A^-}, x_{D^+}, \varepsilon_A, \varepsilon_D) :=}$$

Noting that $F_{D^+}(x_{E^+}, x_{A^-}, x_{D^+}, 0, 0) = r_D x_{E^+} + x_{A^-}$ does not depend on x_{D^+}, it becomes apparent that ε_D and ε_A cannot approach zero simultaneously. Moreover, this demonstrates why multi-scale convergence results such as [17], [38] appear to be not directly applicable.

VI. Numerical Simulations

In this section we apply the PID feedback control architecture developed in this paper to a protein control problem. In particular, we consider a protein, expressed from a gene, and assume that the protein can diffuse between two different compartments according to a passive diffusion model [39].

A. Comparison of PI and PID controllers

The model is composed of the following reactions, where for simplicity we fixed unitary kinetic parameters

$$\begin{aligned} \varnothing &\xrightarrow{1} mRNA & mRNA &\xrightarrow{1} \to\varnothing \\ mRNA &\xrightarrow{1} mRNA + Pro_1 & Pro_1 &\xrightarrow{1} \varnothing \\ Pro_1 &\xrightarrow{1} Pro_2 & Pro_2 &\xrightarrow{1} Pro_1 \\ Pro_2 &\xrightarrow{1} \varnothing. \end{aligned}$$

That is, we have that $mRNA$ catalyses the production of the protein in the first compartment (Pro_1), which can then diffuse in the second compartment (Pro_2) by following its gradient of concentration.

The objective of the control is to have the protein concentration in the second compartment, Pro_2, to follow a reference signal. Given U^+ and U^-, the control signals synthesized by the controller, we assume that these can act on the plant by regulating the expression rate of the $mRNA$. This assumption is justified by the fact that this mechanism can be implemented synthetically. We consider the following reactions to model such actuation:

$$U^+ + mRNA \xrightarrow{l} U^+ + 2mRNA \quad U^- + mRNA \xrightarrow{l} U^-. \tag{8}$$

We note that these satisfy the conditions of Theorem 2.

In this model, a high concentration of U^+ will increase the production rate of $mRNA$ and so of Pro_1 and Pro_2, whereas a high concentration of U^- will decrease the amount of $mRNA$. For our experiments we fix $l = 0.08$. Note that this is an indirect control problem where we cannot act directly on the target species Pro_2, which is the scenario where the derivative component of the PID can be of greater help.

In Figure 3 we compare the performance of PI and PID controllers for various reference signals. In particular, we consider a linear production/degradation model (top left), a pulsed degradation model (top right), a sine wave (bottom left), and a sigmoid (bottom right). For all the tests we consider the same parameters for PI and PID controllers (as reported in the figure caption). It possible to observe that, whereas a negative feedback with a PI controller can already track all signals correctly, in the case of a PID controller the time evolution of the concentration of Pro_2 has reduced oscillations around the reference signals. In all cases, as expected, the time for the convergence of the plant to the reference signal has decreased due to the action of the derivative block.

B. Robustness to Parameter Noise

In Figure 3 we fixed some of the rates of the reactions composing our PID controller to be exactly the same. This was required in Theorem 3 to establish the correctness of the closed loop system. In practice, as discussed in Section IV, the assumption that some of the rates are equal may hold only approximately. As a consequence, in this subsection we empirically evaluate the robustness of our PID architecture when this assumption does not hold exactly.

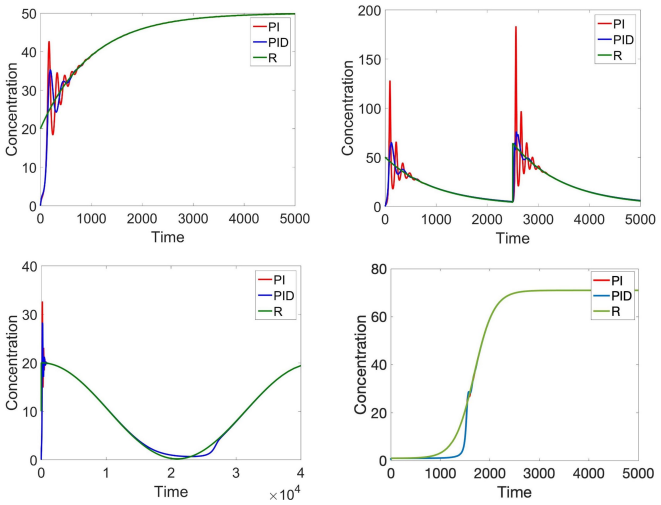

Figure 3: We consider the diffusion model in Section VI and compare the time evolution of the species Pro_2 with different reference signals (green lines) for PID and PI feedback control with the same parameters for all figures ($r_D = 0.05, r_P = 0.025, r_I = 0.0045, s_P = 1, s_M = s_U = s_D = s_A = q = 100$) It is possible to observe that while Pro_2 already tracks correctly the reference signals for PI control, in the case of a PID controller, the output has reduced oscillations around the reference signal.

We consider the same scenario as in Figure 3 and perturb each rate by a value uniformly sampled between $[-\frac{|K|}{2}, \frac{|K|}{2}]$ for $|K| \geq 0$, i.e., each rate is multiplied by factor $(1 + k)$ with $k \in [-\frac{|K|}{2}, \frac{|K|}{2}]$. In the box-plots reported in Figure 4 we plot, for different values of $|K|$, the distribution of the maximum relative error obtained by numerically solving the resulting ODEs system multiple times for each $|K|$ (1000 for each value). The maximum relative error is defined as the maximum of the distance between the reference signal and the output of the plant at time t for $t \in [0, 10000]$, divided by the concentration of the reference signal at time $t = 10000$ (when the system has reached the equilibrium). We note that even relatively large fluctuations of the rates (i.e., $|K| < 0.14$) do not influence significantly the correctness of the system on average. Note also that for $|K| = 0$ the resulting error is not 0. This is because even when the rates are not affect by noise, the PID controller still requires a non-zero amount of time to reach the value of the reference signal.

VII. Conclusions

This work considered feedback control with PID controllers expressed by a novel CRN implementation which computes the derivative of an input molecular signal. We applied our framework to control a gene expression model where a protein can diffuse across different compartments and showed improved performance compared to a PI feedback control. The asymptotic correctness of the biochemical PID controller was established. An interesting aspect, which has not been considered in this paper, is to study the effect that the proposed control system has on noise. This is left as future work.

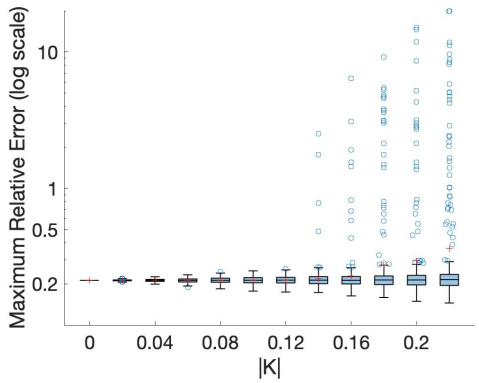

Figure 4: Box plots representing the maximum relative error of our PID controller from Figure 3, while perturbing each rate of our PID controller by a value uniformly sampled between $[-\frac{|K|}{2}, \frac{|K|}{2}]$. For each value of $|K|$ statistics are computed over 1000 different executions of the system. Blue area is the area between first and third quantile, with black horizontal bar being the median. Red cross is the average. Blue dots represents outliers (according to the R-8 method).

ACKNOWLEDGMENT

The authors would like to thank the reviewers for helpful suggestions that improved the quality of the manuscript.

REFERENCES

[1] P. Érdi and J. Tóth, *Mathematical models of chemical reactions: theory and applications of deterministic and stochastic models*. Manchester University Press, 1989.

[2] D. Soloveichik, G. Seelig, and E. Winfree, "DNA as a universal substrate for chemical kinetics," *Proceedings of the National Academy of Sciences*, vol. 107, no. 12, pp. 5393–5398, 2010.

[3] Y.-J. Chen, N. Dalchau, N. Srinivas, A. Phillips, L. Cardelli, D. Soloveichik, and G. Seelig, "Programmable chemical controllers made from DNA," *Nature nanotechnology*, vol. 8, no. 10, p. 755, 2013.

[4] L. Cardelli, M. Češka, M. Fränzle, M. Kwiatkowska, L. Laurenti, N. Paoletti, and M. Whitby, "Syntax-guided optimal synthesis for chemical reaction networks," in *International Conference on Computer Aided Verification*. Springer, 2017, pp. 375–395.

[5] T.-Y. Chiu, H.-J. K. Chiang, R.-Y. Huang, J.-H. R. Jiang, and F. Fages, "Synthesizing configurable biochemical implementation of linear systems from their transfer function specifications," *PloS one*, vol. 10, no. 9, p. e0137442, 2015.

[6] D. Del Vecchio, A. J. Dy, and Y. Qian, "Control theory meets synthetic biology," *Journal of The Royal Society Interface*, vol. 13, no. 120, p. 20160380, 2016.

[7] C. L. Kelly, A. W. K. Harris, H. Steel, E. J. Hancock, J. T. Heap, and A. Papachristodoulou, "Synthetic negative feedback circuits using engineered small RNAs," *Nucleic acids research*, vol. 46, no. 18, pp. 9875–9889, 2018.

[8] N. Barkai and S. Leibler, "Robustness in simple biochemical networks," *Nature*, vol. 387, no. 6636, p. 913, 1997.

[9] U. Alon, L. Camarena, M. G. Surette, B. A. y Arcas, Y. Liu, S. Leibler, and J. B. Stock, "Response regulator output in bacterial chemotaxis," *The EMBO journal*, vol. 17, no. 15, pp. 4238–4248, 1998.

[10] F. Zhang, J. M. Carothers, and J. D. Keasling, "Design of a dynamic sensor-regulator system for production of chemicals and fuels derived from fatty acids," *Nature biotechnology*, vol. 30, no. 4, p. 354, 2012.

[11] M. J. Dunlop, J. D. Keasling, and A. Mukhopadhyay, "A model for improving microbial biofuel production using a synthetic feedback loop," *Systems and synthetic biology*, vol. 4, no. 2, pp. 95–104, 2010.

[12] T.-M. Yi, Y. Huang, M. I. Simon, and J. Doyle, "Robust perfect adaptation in bacterial chemotaxis through integral feedback control," *Proceedings of the National Academy of Sciences*, vol. 97, no. 9, pp. 4649–4653, 2000.

[13] C. Briat, A. Gupta, and M. Khammash, "Antithetic integral feedback ensures robust perfect adaptation in noisy biomolecular networks," *Cell systems*, vol. 2, no. 1, pp. 15–26, 2016.

[14] K. Oishi and E. Klavins, "Biomolecular implementation of linear I/O systems," *IET systems biology*, vol. 5, no. 4, pp. 252–260, 2011.

[15] L. Cardelli, "Two-domain DNA strand displacement," *Mathematical Structures in Computer Science*, vol. 23, no. 2, pp. 247–271, 2013.

[16] F. C. Simmel, B. Yurke, and H. R. Singh, "Principles and applications of nucleic acid strand displacement reactions," *Chemical reviews*, vol. 119, no. 10, pp. 6326–6369, 2019.

[17] F. Verhulst, *Methods and Applications of Singular Perturbations*. Springer, 2005.

[18] M. Whitby, L. Cardelli, M. Kwiatkowska, L. Laurenti, M. Tribastone, and M. Tschaikowski, "PID control of biochemical reaction networks," in *CDC*, 2019, pp. 8372–8379.

[19] M. Kaern, T. C. Elston, W. J. Blake, and J. J. Collins, "Stochasticity in gene expression: from theories to phenotypes," *Nature Reviews Genetics*, vol. 6, no. 6, pp. 451–464, 2005.

[20] L. Laurenti, A. Csikasz-Nagy, M. Kwiatkowska, and L. Cardelli, "Molecular filters for noise reduction," *Biophysical Journal*, vol. 114, no. 12, pp. 3000–3011, 2018.

[21] C. Briat, A. Gupta, and M. Khammash, "Antithetic proportional-integral feedback for reduced variance and improved control performance of stochastic reaction networks," *Journal of The Royal Society Interface*, vol. 15, no. 143, p. 20180079, 2018.

[22] W. Halter, Z. A. Tuza, and F. Allgöwer, "Signal differentiation with genetic networks," *IFAC-PapersOnLine*, vol. 50, no. 1, pp. 10 938–10 943, 2017.

[23] W. Halter, R. M. Murray, and F. Allgöwer, "Analysis of primitive genetic interactions for the design of a genetic signal differentiator," *Synthetic Biology*, vol. 4, no. 1, 2019.

[24] C. C. Samaniego, G. Giordano, and E. Franco, "Practical differentiation using ultrasensitive molecular circuits," in *ECC*, 2019, pp. 692–697.

[25] M. Chevalier, M. Gomez-Schiavon, A. H. Ng, and H. El-Samad, "Design and analysis of a proportional-integral-derivative controller with biological molecules," *Cell Systems*, vol. 9, no. 4, pp. 338–353, 2019.

[26] N. M. G. Paulino, M. Foo, J. Kim, and D. G. Bates, "Pid and state feedback controllers using dna strand displacement reactions," *IEEE Control Systems Letters*, vol. 3, no. 4, pp. 805–810, 2019.

[27] S. Modi, S. Dey, and A. Singh, "Proportional and derivative controllers for buffering noisy gene expression," in *CDC*, 2019, pp. 2832–2837.

[28] L. Cardelli, "Morphisms of reaction networks that couple structure to function," *BMC systems biology*, vol. 8, no. 1, p. 84, 2014.

[29] K. Montagne, G. Gines, T. Fujii, and Y. Rondelez, "Boosting functionality of synthetic dna circuits with tailored deactivation," *Nature communications*, vol. 7, no. 1, pp. 1–12, 2016.

[30] B. Yurke, A. J. Turberfield, A. P. Mills, F. C. Simmel, and J. L. Neumann, "A dna-fuelled molecular machine made of dna," *Nature*, vol. 406, no. 6796, pp. 605–608, 2000.

[31] D. Soloveichik, G. Seelig, and E. Winfree, "Dna as a universal substrate for chemical kinetics," *Proceedings of the National Academy of Sciences*, vol. 107, no. 12, pp. 5393–5398, 2010.

[32] R. M. Dirks, J. S. Bois, J. M. Schaeffer, E. Winfree, and N. A. Pierce, "Thermodynamic analysis of interacting nucleic acid strands," *SIAM review*, vol. 49, no. 1, pp. 65–88, 2007.

[33] N. Srinivas, J. Parkin, G. Seelig, E. Winfree, and D. Soloveichik, "Enzyme-free nucleic acid dynamical systems," *Science*, vol. 358, no. 6369, 2017.

[34] K. M. Cherry and L. Qian, "Scaling up molecular pattern recognition with dna-based winner-take-all neural networks," *Nature*, vol. 559, no. 7714, pp. 370–376, 2018.

[35] Y. Lyu, C. Wu, C. Heinke, D. Han, R. Cai, I.-T. Teng, Y. Liu, H. Liu, X. Zhang, Q. Liu *et al.*, "Constructing smart protocells with built-in dna computational core to eliminate exogenous challenge," *Journal of the American Chemical Society*, vol. 140, no. 22, pp. 6912–6920, 2018.

[36] L. M. Hochrein, T. J. Ge, M. Schwarzkopf, and N. A. Pierce, "Signal transduction in human cell lysate via dynamic rna nanotechnology," *ACS synthetic biology*, vol. 7, no. 12, pp. 2796–2802, 2018.

[37] V. B. Pinheiro, A. I. Taylor, C. Cozens, M. Abramov, M. Renders, S. Zhang, J. C. Chaput, J. Wengel, S.-Y. Peak-Chew, S. H. McLaughlin *et al.*, "Synthetic genetic polymers capable of heredity and evolution," *Science*, vol. 336, no. 6079, pp. 341–344, 2012.

[38] P. T. Cardin and M. A. Teixeira, "Fenichel theory for multiple time scale singular perturbation problems," *SIAM J. Appl. Dyn. Syst.*, vol. 16, no. 3, pp. 1425–1452, 2017.

[39] L. Cardelli, L. Laurenti, and A. Csikasz-Nagy, "Coupled membrane transporters reduce noise," *Phys. Rev. E*, vol. 101, p. 012414, Jan 2020.